
PARD: Accelerating LLM Inference with Low-Cost PArallel Draft Model Adaptation

Zihao An^{1*} Buajun Bai^{1,2*} Ziqiong Liu¹ Dong Li¹ Emad Barsoum¹

¹Advanced Micro Devices, Inc. ²Tsinghua University

{Zihao.An, Huajun.Bai, Ziqiong.Liu, d.li, Emad.Barsoum}@amd.com

Abstract

The autoregressive nature of large language models (LLMs) limits inference speed. Each forward pass generates only a single token and is often bottlenecked by memory bandwidth. Speculative decoding alleviates this issue using a draft-then-verify approach to accelerate token generation. However, the overhead introduced during the draft phase and the training cost of the draft model limit the efficiency and adaptability of speculative decoding. In this work, we introduce PArallel Draft (PARD), a novel speculative decoding method that enables low-cost adaptation of autoregressive draft models into parallel draft models. PARD enhances inference efficiency by predicting multiple future tokens in a single forward pass of the draft phase, and incorporates a conditional drop token method to accelerate training. Its target-independence property allows a single draft model to be applied to an entire family of different models, minimizing the adaptation cost. Our proposed conditional drop token method can improves draft model training efficiency by **3x**. On our optimized inference framework, PARD accelerates LLaMA3.1-8B inference by **4.08x**, achieving **311.5** tokens per second ².

1 Introduction

Rapid advancements in LLMs such as GPT-4 [41], LLaMA3 [35] and DeepSeek-R1 [11] have fueled an explosion of applications such as content generation, code generation, and AI agents. However, as the counts of model parameters and the lengths of the context continue to grow, inference efficiency has become a critical challenge. Due to the auto-regressive (AR) nature of LLMs, tokens are generated sequentially, leading to substantial memory bandwidth consumption and high inference latency.

Speculative Decoding (SD) [5, 25] has emerged as a promising technique to mitigate bandwidth overhead and reduce decoding latency during LLM inference. The core idea is to use a lightweight draft model to predict multiple candidate tokens, which are then verified in parallel by the target model. When combined with speculative sampling, this approach allows the model to generate multiple tokens within a single forward pass, significantly improving efficiency without compromising output quality.

The effectiveness of SD is determined by both the accuracy of the draft model and the overhead it introduces. To improve draft model accuracy, various methods have been proposed, primarily falling into the category of *target-dependent* approaches, where the draft model leverages information from the target model. For example, Medusa [3] and EAGLE [26] incorporate features from the target model’s outputs into the draft model’s input, while LayerSkip [12] and Kangaroo [33] reuse selected layers of the target model as the draft model. Although these methods improve token prediction accuracy, they also introduce a major drawback: the draft model becomes tightly coupled with the

*Equal contribution.

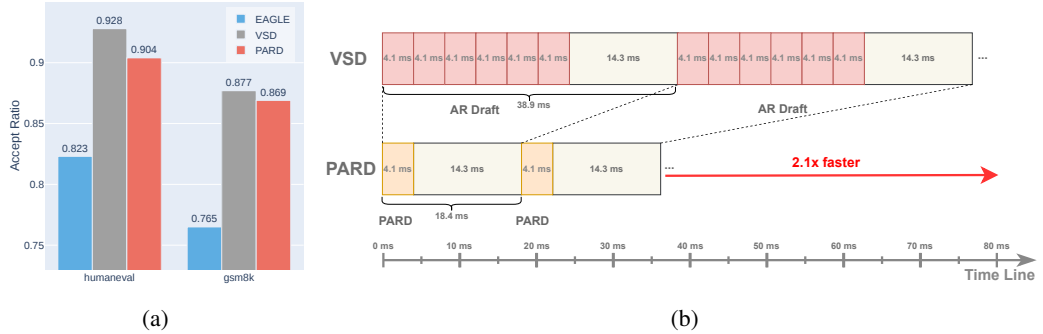


Figure 1: PARD achieves low latency while maintaining high accuracy. (a) Comparison of first-token acceptance rates using LLaMA3-8B as the target model. EAGLE uses the official model, vanilla speculative decoding (VSD) employs LLaMA3.2-1B as the draft model, and PARD represents the adaptive version of VSD. (b) Comparison of actual inference time between VSD and PARD. VSD generates candidate tokens autoregressively during the draft stage, requiring multiple forward passes. In contrast, PARD completes drafting with a single forward pass. The draft model used is LLaMA3.2-1B and the target model is LLaMA3-8B.

target model. Consequently, different target model versions require separately trained draft models, increasing adaptation and deployment costs.

Alternatively, mask prediction [17] provides a form of parallel decoding by using masked tokens as placeholders and employing specialized training to enable multiple token predictions in a single forward pass. Several recent studies have integrated speculative decoding with mask prediction. For example, PaSS [39] and BiTA [18] fine-tune the target model into a parallel decoding model that functions as a draft model, while ParallelSpec [50] extends EAGLE and Medusa into a parallel decoding framework. However, these approaches still rely on target model information, making them inherently target-dependent.

Unlike target-dependent methods, vanilla SD [5, 25] represents a class of *target-independent* approaches, where a single draft model can be applied across an entire family of target models without requiring separate training for each variant. To evaluate the effectiveness of this approach, we compared using LLaMA3.2-1B [35] as a draft model against the EAGLE method for the target model LLaMA3-8B. As shown in Figure 1a, our results show that LLaMA3.2-1B achieves significantly higher accuracy than the EAGLE head. However, due to its increased computational cost the overall speedup ratio was lower than that of EAGLE.

To address the limitations of existing methods, we propose Parallel Draft (**PARD**), a novel speculative decoding approach. PARD builds upon existing high-accuracy small language models. It enhances them with minimal adaptation training, enabling parallel decoding. PARD maintains high accuracy while significantly reducing inference latency. Unlike target-dependent methods, PARD is a *target-independent* approach. A single trained draft model can be applied across an entire family of target models. This significantly reduces adaptation costs.

To reduce training costs during adaptation, we introduce a conditional drop token training strategy, where certain training tokens are selectively dropped under specific constraints. This strategy improves training speed by 3 \times while preserving model accuracy.

To align our evaluation with real-world scenarios, we optimize the Transformers library and develop a performance-optimized version called Transformers+. Both the baseline and SD methods achieve over 2x additional speedup on Transformers+, and PARD is designed to be easy to use with fewer than 500 lines of code. Moreover, we integrate PARD into vLLM, and conduct all experiments on Transformers+ and vLLM.

We evaluate PARD on three model families: LLaMA3, Deepseek-R1-Distilled, and Qwen, demonstrating a $1.78\times$ speedup over vanilla SD. Notably, for Qwen2.5 7B, PARD achieves up to $4.87\times$ acceleration, reaching a token generation speed of 381.7 tokens per second.

To summarize, we make the following contributions:



Figure 2: AR and AR+ represent baseline auto-regressive generation using Transformers and Transformers+, respectively. VSD denotes vanilla speculative decoding, where the draft models used are LLaMA3.2-1B, DeepSeek-R1-Qwen-1.5B, and Qwen2.5-0.5B. PARD refers to the proposed method in this paper. The results for Qwen and LLaMA3 are based on the HumanEval benchmark, while DeepSeek was evaluated on the reasoning task MATH500.

- We propose PARD, a novel speculative decoding method that enables low-cost adaptation of AR draft models into parallel draft models. Compared to AR draft models, PARD achieves an average inference speedup of 1.78 \times . By proposing a conditional drop token strategy, PARD improves training efficiency by up to 3 \times while maintaining accuracy.
- PARD is generalizable: its target-independent design allows a single draft model to accelerate an entire family of target models, in contrast to target-dependent methods like Medusa and EAGLE. In this way, PARD significantly reduces deployment and adaptation costs.
- We integrate PARD into an optimized inference framework called Transformers+ and achieve up to 4.08 \times speedup, with LLaMA3.1 8B reaching a state-of-the-art 311.5 tokens per second on an A100-40GB GPU. When integrated into vLLM, PARD delivers up to 3.06 \times speedup, outperforming other speculative decoding methods in vLLM by 1.51 \times .

2 Preliminaries

2.1 Auto-Regressive Nature of LLMs

Modern LLMs are based on the GPT architecture [42]. During the training phase, GPT models leverage highly efficient parallelization, allowing tokens within a sequence to be processed simultaneously. This parallelism enables GPUs to fully utilize computational resources by maximizing matrix multiplications and optimizing memory bandwidth usage, thereby improving training efficiency. Given an input sequence $X = (x_0, x_1, \dots, x_{N-1})$ and its corresponding target sequence $Y = (x_1, x_2, \dots, x_N)$, the training objective of GPT is to minimize the auto-regressive loss, which can be expressed as:

$$\mathcal{L} = - \sum_{t=1}^N \log P(x_t | x_0, \dots, x_{t-1}). \quad (1)$$

However, during inference, due to its auto-regressive nature, GPT must generate tokens sequentially, with each token depending on all previously generated tokens. This sequential generation process leads to a significant drop in computational efficiency. At each step t , the model computes:

$$x_t = \arg \max P(x_t | x_0, \dots, x_{t-1}). \quad (2)$$

This sequential generation results in a memory-bound scenario, where GPU performance is constrained by the repeated loading of model weights and the KV-cache, rather than being fully utilized for large-scale parallel computations. As a result, even though GPUs are capable of high-speed matrix multiplications, the decoding phase remains bottlenecked by memory access latency, leading to high latency during the decoding phase.

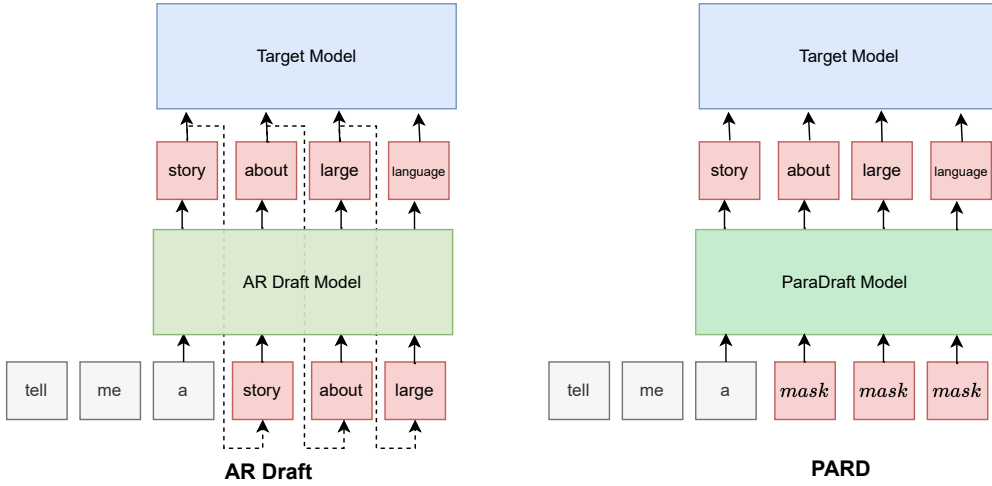


Figure 3: Illustration of PARD Inference. *Left*: Vanilla speculative decoding involves a draft model auto-regressively generating K candidate tokens, which are then validated by the target model in parallel. *Right*: PARD introduces mask tokens for parallel Draft. All K candidate tokens are generated in one forward pass.

2.2 Speculative Decoding

SD can effectively reduce decoding latency and improve matrix multiplication efficiency. The core idea behind SD is to first use a smaller draft model to generate a set of candidate tokens, and then use the target model to verify the candidates. The process is as follows:

Drafting Stage: The goal of this stage is to generate the next K candidate tokens $C = (x'_n, \dots, x'_{n+K-1})$. These candidates can be produced by a lightweight model or traditional machine learning algorithms. For the vanilla SD method, the draft model generates the K candidates auto-regressively.

Verification Stage: The target model then verifies the candidate tokens in parallel, improving computational efficiency. When combined with speculative sampling, SD ensures no loss of performance.

We define T_D as the time taken by the draft model for a single forward pass, and T_T as the time taken by the target model for a single forward pass. The input length to both the draft and target models can vary across different SD methods. However, when the input length is not significantly large, the change in speed is negligible. For simplicity, we use T_D and T_T to represent the time taken by the draft and target models, respectively. For the vanilla SD method, the time taken per iteration is:

$$T_{\text{AR}_{\text{draft}}} = K * T_D + T_T. \quad (3)$$

As shown in Figure 1b, when using a high acceptance rate model like LLaMA3.2-1B to accelerate LLaMA3.2-8B, the draft model consumes a considerable amount of time. Our PARD method fine-tunes the draft model into a parallel decoding model. In this case, the time taken is:

$$T_{\text{PARD}} = T_D + T_T. \quad (4)$$

It can be seen that PARD reduces the total time of the draft model to $1/K$ of the original time, significantly lowering the overall decoding time.

3 PARD Framework

We begin by introducing how the PARD model predicts multiple tokens in a single forward pass and provide a detailed explanation of its inference process in Section 3.1. Next in Section 3.2, we describe how to finetune a vanilla draft model to acquire the capabilities of PARD. Moreover, we propose a conditional drop training token method that significantly accelerates training.

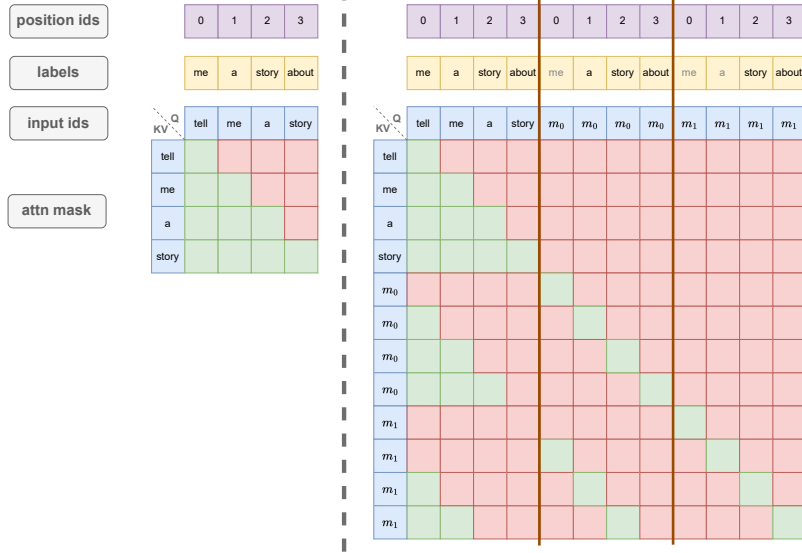


Figure 4: Illustration of PARD training. The *left* figure illustrates the training data for a standard autoregressive model. *Right* figure represents the training data for PARD. The diagram is divided into three sections by solid lines, corresponding to training objectives for predicting tokens at positions +1, +2, and +3. The designed attention mask ensures consistency between training and inference. Labels in lighter font indicate tokens that are supplemented for context completion and do not contribute to the loss computation.

3.1 PARD Inference

The objective of the draft model θ is to predict the next K tokens by optimizing the probability distribution:

$$P(x_n, \dots, x_{n+K-1} | x_0, \dots, x_{n-1}; \theta). \quad (5)$$

For the vanilla speculative decoding method, this probability can be factorized as:

$$P(x_n, \dots, x_{n+K-1} | x_0, \dots, x_{n-1}; \theta_{\text{AR}_{\text{draft}}}) = \prod_{k=0}^{K-1} P(x_{n+k} | x_0, \dots, x_{n+k-1}; \theta_{\text{AR}_{\text{draft}}}). \quad (6)$$

This formulation follows the standard autoregressive approach in Figure 3, where each token is generated sequentially based on all previously predicted tokens.

In contrast, PARD introduces a special token m_k as a placeholder to replace tokens that would otherwise create dependencies. The formulation is as follows:

$$P(x_n, \dots, x_{n+K-1} | x_0, \dots, x_{n-1}, \theta_{\text{PARD}}) = \prod_{k=0}^{K-1} P(x_{n+k} | x_0, \dots, x_{n-1}, m_0, \dots, m_{k-1}; \theta_{\text{PARD}}). \quad (7)$$

As shown in the equation, the predictions at each step do not depend on each other, enabling fully parallel inference. This reduces the number of forward passes required by the draft model from K to 1, significantly improving inference efficiency.

3.2 PARD Training

To enable the vanilla draft model to predict multiple tokens within a single forward pass, we adopt a mask token training strategy which adapts a standard auto-regressive draft model into a parallel draft model. Additionally, we propose an efficient conditional drop training token strategy, which significantly improves training efficiency while maintaining final performance.

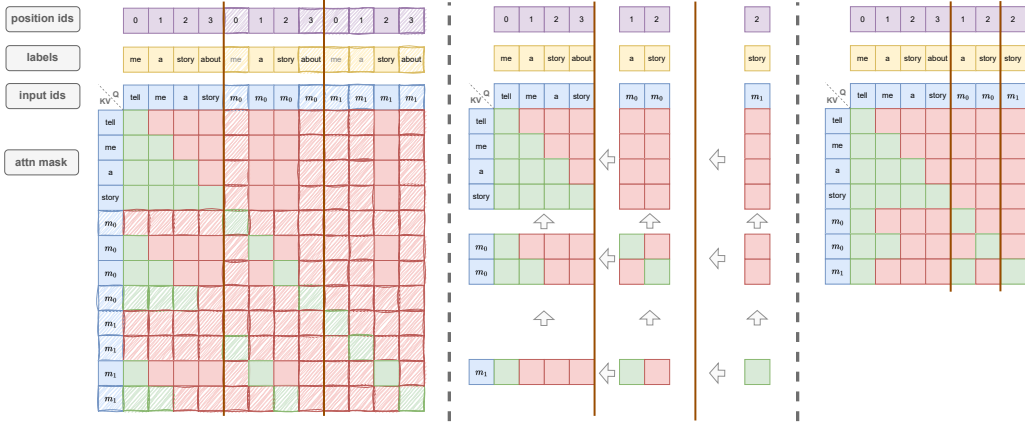


Figure 5: Illustration of Conditional Drop in PARD training. *Left*: The retention pattern follows a geometric decay where a fraction $r = 0.5$ of positions is retained for mask token m_0 and $r^2 = 0.25$ for m_1 , ensuring that each retained token maintains complete preceding key-value (KV) pairs. *Middle*: The resulting sparse attention structure after applying Conditional Drop. *Right*: The sparse matrix reorganized into a compact format by eliminating dropped positions.

3.2.1 Mask Tokens based Training

To ensure consistency between the training and inference processes, we divide training into multiple independent subtasks, where each subtask is designed to predict x_n, \dots, x_{n+K-1} . As shown in Figure 4, these subtasks can be trained simultaneously with minimal preprocessing of the training data. The loss for each subtask is computed using a cross-entropy function, as follows:

$$\mathcal{L}_k = -\frac{1}{N-k+1} \sum_{i=k}^N \log P(x_i|x_0, x_1, \dots, x_{i-1}, m_0, \dots, m_{k-2}; \theta_{\text{PARD}}). \quad (8)$$

where \mathcal{L}_k represents the loss function for predicting the k -th next token, and N denotes the length of the sample.

Compared to standard auto-regressive model training, the mask token training method breaks the task into multiple subtasks, significantly increasing the training cost. For example, if the training sample length is N , then the number of tokens for AR training is also N . However, in the mask token training approach, the number of tokens for training increases from N to $K \times N$, where K is the number of tokens the draft model predicts simultaneously in a single forward pass.

To address this challenge, we propose an innovative COnditional Drop training token (COD) strategy. This method boosts training efficiency significantly while maintaining prediction accuracy. The core idea behind COD is that tokens in earlier subtasks are more critical, whereas those in later subtasks can be selectively dropped to reduce computation.

During the token dropping process, we ensure that the remaining tokens still provide complete key and value information when computing attention, thereby preserving the essential contextual information, as illustrated in Figure 5. Even though some tokens are dropped, the key contextual representations remain intact.

3.2.2 Conditional Drop of Training Tokens

To manage the number of tokens retained for each subtask, we introduce a retention parameter r . For the i -th subtask, the number of retained tokens N_i is given by:

$$N_i = N * r^{i-1}. \quad (9)$$

Consequently, the total number of training tokens can be expressed as:

$$N_{\text{COD}} = \sum_{i=1}^K N_i = \sum_{i=1}^K N * r^{i-1} = N \frac{1 - r^K}{1 - r} < \frac{N}{1 - r}. \quad (10)$$

For instance, when $r = 0.5$, the number of training tokens can be reduced from $K \times N$ to $2N$, significantly lowering the training cost. Additionally, to prevent excessive token dropping in later subtasks, we introduce a minimum retention ratio r_{min} , ensuring that the retention rate does not fall below a predefined threshold. The adjusted number of retained tokens for each subtask is:

$$N'_i = N * \max(r^{i-1}, r_{min}). \quad (11)$$

The detailed algorithm for COD with all applied methods is described in Algorithm 1. By using the COD strategy, the training cost of PARD can be significantly reduced.

Algorithm 1 PARD with Conditional Drop Tokens: Data Processing

```

1: Input: Training dataset  $\mathcal{D}$ , PARD prediction count  $K$ , retention decay factor  $r$ , minimum
   retention rate  $r_{min}$ 
2: Output: Processed training data with updated input_ids, labels, position encodings, and attention
   masks
3: for each data sample  $X \in \mathcal{D}$  do
4:    $X \leftarrow [X_1, \dots, X_K]$ , where  $X_k$  is the training data for predicting the  $k$ -th token, including
   input ids, label, position ids, and attention mask
5:   for  $k = 1$  to  $K$  do
6:     Compute retention rate:  $\gamma \leftarrow \max(r^{k-1}, r_{min})$ 
7:     Decide which tokens in  $X_k$  to retain, ensuring that the preceding KV cache for attention
   computation is complete
8:     Update  $X_k$  (i.e., input ids, label, position ids, and attention mask) to obtain  $X'_k$ 
9:   end for
10:  Merge updated sequences  $X' \leftarrow [X'_1, \dots, X'_K]$  and update the overall attention mask
11:  Store the processed data for this sample
12: end for

```

4 Evaluation

4.1 Experimental Setup

Models: We conduct experiments on popular industry models, including LLaMA3 [19], DeepSeek-R1-Qwen [20], and Qwen [52]. For each model series, we select the smallest model variant and train it in the PARD framework.

Datasets: To ensure alignment with the original instruct model training process, we select datasets tailored to each model series. LLaMA3 is trained with Magpie-Llama-3.1-Pro-1M [51] and Evol-CodeAlpaca [37]. Qwen2.5 is trained with Magpie-Qwen2-Pro-1M and Evol-CodeAlpaca. DeepSeekR1Qwen is trained with OpenR1-Math-220k [13], OpenThoughts-114k [45], and Chinese-DeepSeek-R1-Distill-Data-110k [32]. For LLaMA 3 and Qwen, we further enhance training accuracy by regenerating answers.

Tasks: We evaluate the effectiveness of PARD on mathematical reasoning and code generation tasks on benchmarks including HumanEval [7], GSM8K [9] and MATH500 [29].

Training: We conduct training on 8xMI250X cards using the TRL framework for a total of 4 epochs. During training, the parameters are set as follows: $k = 8$, $r = 0.7$, and $r_{min} = 0.2$.

Evaluation: To maximize GPU bandwidth utilization and approach its upper limit, we upgrade the transformers [46] framework with optimizations like `torch.compile` and `kvcache`, resulting in `transformers+`. All tests are conducted using this high-performance framework. The evaluation is performed on a single A100-40GB GPU.

Metrics:

Tokens Per Second: The number of tokens generated per second in real-world scenarios.

Speedup: The acceleration ratio compared to the baseline standard auto-regressive generation method. Here, we use the `transformer+` version as a high-performance baseline.

4.2 Experimental Results

Table 1 compares the acceleration effects of PARD on mainstream models with 7B and 8B parameters. First, our optimized baseline `transformers+` (AR+) achieves more than $2\times$ speedup compared to the unoptimized AR. PARD further accelerates inference by $2.5 \sim 4.9\times$ compared to AR+ and achieves a $1.78\times$ improvement over vanilla speculative decoding. The maximum throughput reaches **381.7** tokens per second on a single A100-40GB GPU. All tests are conducted using chain decoding.

Our experiments further demonstrate the **target independence** property of PARD, where a single PARD model can accelerate an entire series of target models in Table 2. Specifically, we evaluate four target models from the LLaMA3 series, three target models from DeepSeek-R1, and seven target models from Qwen. PARD achieves a speedup of **1.76×** over vanilla SD. Additionally, we observe that when the draft and target models are of the same size, PARD still provides a $2.1\times$ speedup on the MATH500 dataset.

Table 1: AR and AR+ represent baseline autoregressive generation using Transformers and Transformers+ respectively. The target models include LLaMA3.1-8B (L3.1 8B), DeepSeek-R1-Distill-Qwen-7B (DSQ 7B), and Qwen2.5-7B (Q2.5 7B). The draft models used are LLaMA3.2-1B (L3.2 1B), DeepSeek-R1-Distill-Qwen-1.5B (DSQ 1.5B), and Qwen2.5-0.5B (Q2.5 0.5B). We compare each draft model before and after PARD adaptation to evaluate efficiency gains. The temperature is set to 0 for all experiments.

Target	Method	Draft	MATH500		HumanEval		GSM8K		Average	
			TPS	Speedup	TPS	Speedup	TPS	Speedup	TPS	Speedup
L3.1 8B	AR	-	35.4	0.46x	35.2	0.46x	35.5	0.46x	35.4	0.46x
	AR+	-	77.0	1.00x	76.4	1.00x	76.9	1.00x	76.8	1.00x
	VSD	L3.2 1B	176.6	2.29x	183.4	2.40x	171.4	2.23x	177.1	2.31x
	PARD	L3.2 1B PARD	258.0	3.35x	311.5	4.08x	253.7	3.30x	274.4	3.57x
DSQ 7B	AR	-	39.0	0.49x	38.8	0.49x	38.6	0.49x	38.8	0.49x
	AR+	-	79.3	1.00x	79.3	1.00x	79.4	1.00x	79.3	1.00x
	VSD	DSQ 1.5B	120.0	1.51x	109.1	1.38x	123.6	1.56x	117.6	1.48x
	PARD	DSQ 1.5B PARD	253.8	3.20x	195.0	2.46x	231.2	2.91x	226.7	2.86x
Q2.5 7B	AR	-	40.0	0.51x	39.7	0.52x	39.7	0.51x	39.8	0.51x
	AR+	-	78.0	1.00x	75.9	1.00x	78.3	1.00x	77.4	1.00x
	VSD	Q2.5 0.5B	187.9	2.41x	169.4	2.23x	195.3	2.49x	184.2	2.38x
	PARD	Q2.5 0.5B PARD	315.6	4.04x	356.3	4.69x	381.7	4.87x	351.2	4.54x

4.3 Ablation Studies

For all ablation study experiments, the target model used is DeepSeek-R1-Qwen-7B, and the draft model’s pretraining model is DeepSeek-R1-Qwen-1.5B. Training is conducted on a 93K subset of OpenR1-Math-220K for one epoch, and testing is performed using the MATH500 dataset.

Conditional Drop Token: The lower the retention rate, the greater the acceleration effect. However, excessively low retention may degrade model performance. As shown in 6a, when setting $r = 0.7$ and $r_{\min} = 0.2$, we achieve a good balance between speed and accuracy. This setting allows us to achieve $3\times$ faster training while maintaining the original accuracy. All experiments in this paper adopt these parameters.

Shared Mask Token ID Strategy: We compare different prediction strategies and find that using the same mask token ID across all predicted positions, i.e., $m_0 = m_1 = \dots = m_{K-1}$, performs better than using distinct token IDs. The corresponding throughput results are 221.97 and 218.05 tokens/s, respectively. This approach not only improves prediction consistency but also enhances the model’s ability to generalize beyond its training configuration, a property we refer to as *extrapolation capability*. Specifically, extrapolation capability allows the model to infer with a larger K during inference than it was trained on.

Selection of Draft K : We conduct a Cartesian product test for K_{train} during training and K_{infer} during inference in Figure 6b. Due to the extrapolation capability of PARD enabled by the shared mask token ID, K_{infer} can be greater than K_{train} . The best performance is achieved at $K_{\text{infer}} = 12$, while results remain stable when $K_{\text{train}} \geq 8$. Therefore, we select $K_{\text{train}} = 8$.

Table 2: The target models include LLama3-8B (L3 8B), LLama3.2-1B (L32 1B), LLama3.2-3B (L32 3B), LLama3.1-8B (L31 8B), DeepSeek-R1-Distill-Qwen-1.5B (DSQ 1.5B), DeepSeek-R1-Distill-Qwen-7B (DSQ 7B), DeepSeek-R1-Distill-Qwen-14B (DSQ 14B), Qwen2-7B (Q2 7B), Qwen2.5-1.5B (Q2.5 1.5B), Qwen2.5-3B (Q2.5 3B), Qwen2.5-7B (Q2.5 7B), Qwen2.5-14B (Q2.5 14B), and Qwen2.5-7B-1M (Q2.5 7B 1M). The draft models used are LLama3.2-1B (L32 1B), DeepSeek-R1-Distill-Qwen-1.5B (DSQ 1.5B), Qwen2.5-0.5B (Q2.5 0.5B), and their PARD-adapted versions. AR+ represents baseline autoregressive generation using Transformers+. The temperature is set to 0 for all experiments.

Series	Target	Method	Draft	MATH500		HumanEval		GSM8K		Average	
				TPS	Speedup	TPS	Speedup	TPS	Speedup	TPS	Speedup
L3	L3 8B	AR+	-	77.3	1.00x	75.7	1.00x	75.9	1.00x	76.3	1.00x
		VSD	L32 1B	154.2	1.99x	187.1	2.47x	150.0	1.98x	163.8	2.15x
		PARD	L32 1B PARD	234.4	3.03x	301.1	3.98x	208.7	2.75x	248.0	3.25x
	L32 1B	AR+	-	316.3	1.00x	314.4	1.00x	315.7	1.00x	315.5	1.00x
		VSD	L32 1B	231.6	0.73x	305.4	0.97x	296.3	0.94x	277.8	0.88x
		PARD	L32 1B PARD	654.3	2.07x	749.5	2.38x	646.3	2.05x	683.4	2.17x
	L32 3B	AR+	-	147.5	1.00x	147.4	1.00x	146.8	1.00x	147.2	1.00x
		VSD	L32 1B	224.3	1.52x	231.6	1.57x	213.4	1.45x	223.1	1.52x
		PARD	L32 1B PARD	407.7	2.76x	446.7	3.03x	385.3	2.63x	413.2	2.81x
	L31 8B	AR+	-	77.0	1.00x	76.4	1.00x	76.9	1.00x	76.8	1.00x
		VSD	L32 1B	176.6	2.29x	183.4	2.40x	171.4	2.23x	177.1	2.31x
		PARD	L32 1B PARD	258.0	3.35x	311.5	4.08x	253.7	3.30x	274.4	3.57x
DSQ	DSQ 1.5B	AR+	-	221.0	1.00x	222.2	1.00x	222.2	1.00x	221.8	1.00x
		VSD	DSQ 1.5B	193.1	0.87x	189.7	0.85x	194.8	0.88x	192.5	0.87x
		PARD	DSQ 1.5B PARD	455.2	2.06x	371.9	1.67x	424.8	1.91x	417.3	1.88x
	DSQ 7B	AR+	-	79.3	1.00x	79.3	1.00x	79.4	1.00x	79.3	1.00x
		VSD	DSQ 1.5B	120.0	1.51x	109.1	1.38x	123.6	1.56x	117.6	1.48x
		PARD	DSQ 1.5B PARD	253.8	3.20x	195.0	2.46x	231.2	2.91x	226.7	2.86x
	DSQ 14B	AR+	-	41.5	1.00x	41.6	1.00x	41.7	1.00x	41.6	1.00x
		VSD	DSQ 1.5B	91.9	2.22x	83.6	2.01x	96.3	2.31x	90.6	2.18x
		PARD	DSQ 1.5B PARD	149.3	3.60x	110.4	2.66x	135.8	3.26x	131.8	3.17x
	Q2 7B	AR+	-	79.4	1.00x	79.6	1.00x	79.5	1.00x	79.5	1.00x
		VSD	Q2.5 0.5B	140.7	1.77x	154.3	1.94x	155.4	1.95x	150.1	1.89x
		PARD	Q2.5 0.5B PARD	238.6	3.00x	291.7	3.66x	255.1	3.21x	261.8	3.29x
Qwen	Q2.5 1.5B	AR+	-	223.0	1.00x	224.2	1.00x	224.6	1.00x	223.9	1.00x
		VSD	Q2.5 0.5B	251.8	1.13x	227.9	1.02x	263.7	1.17x	247.8	1.11x
		PARD	Q2.5 0.5B PARD	512.2	2.30x	579.1	2.58x	570.0	2.54x	553.8	2.47x
	Q2.5 3B	AR+	-	139.0	1.00x	140.0	1.00x	140.5	1.00x	139.8	1.00x
		VSD	Q2.5 0.5B	231.8	1.67x	227.6	1.63x	241.3	1.72x	233.6	1.67x
		PARD	Q2.5 0.5B PARD	387.3	2.79x	485.1	3.46x	460.5	3.28x	444.3	3.18x
	Q2.5 7B	AR+	-	78.0	1.00x	75.9	1.00x	78.3	1.00x	77.4	1.00x
		VSD	Q2.5 0.5B	187.9	2.41x	169.4	2.23x	195.3	2.49x	184.2	2.38x
		PARD	Q2.5 0.5B PARD	315.6	4.04x	356.3	4.69x	381.7	4.87x	351.2	4.54x
	Q2.5 14B	AR+	-	41.8	1.00x	41.9	1.00x	42.0	1.00x	41.9	1.00x
		VSD	Q2.5 0.5B	148.4	3.55x	130.4	3.11x	152.0	3.62x	143.6	3.43x
		PARD	Q2.5 0.5B PARD	185.7	4.44x	215.1	5.13x	225.8	5.38x	208.9	4.98x
	Q2.5 7B 1M	AR+	-	79.6	1.00x	79.8	1.00x	79.7	1.00x	79.7	1.00x
		VSD	Q2.5 0.5B	178.1	2.24x	149.6	1.87x	182.7	2.29x	170.2	2.14x
		PARD	Q2.5 0.5B PARD	303.2	3.81x	311.4	3.90x	343.4	4.31x	319.3	4.01x

Comparison with the Mainstream Method EAGLE: For SD, higher acceptance ratio combined with lower bandwidth consumption results in superior speedup. In Table 5 and Table 6, we compare PARD and EAGLE. PARD achieves a higher acceptance ratio while consuming less bandwidth.

Mainstream Inference Frameworks and Large Batch Size Inference: We have integrated PARD into the vLLM framework. Table 3 compares the speedup effects of PARD, EAGLE, and vanilla SD, with PARD achieving a 2.80x to 3.06x speedup. Table 4 further presents results across batch sizes ranging from 1 to 16. As the batch size increases, the bottleneck shifts from memory-bound to compute-bound. Under these conditions, PARD achieves a speedup of 1.17x to 3.06x. For each setup in vLLM, we select the optimal K_{infer} to ensure fair comparison.



Figure 6: (a) Compare the effects of different values of r and r_{\min} , where each experiment is labeled as $\text{PARD}_r r_{\min}$. The x-axis represents training time, while the y-axis indicates the final decoding speed. (b) presents the results under different K_{train} and K_{infer} settings. The x-axis represents K_{infer} , and the experiment names $\text{PARD}_K K_{\text{train}}$ denote different K_{train} values.

Table 3: Comparison of speculative decoding methods on LLaMA3-8B in the vLLM framework, evaluated with batch size = 1.

Method	HumanEval		GSM8K	
	TPS	Speedup	TPS	Speedup
AR	71.0	1.00x	71.2	1.00x
EAGLE	116.6	1.64x	107.6	1.51x
VSD	143.4	2.02x	136.5	1.92x
PARD	217.6	3.06x	199.6	2.80x

Table 4: Performance comparison across different batch sizes on LLaMA3-8B in the vLLM framework, evaluated on HumanEval.

Method	bs=1	bs=2	bs=4	bs=8	bs=16
	Speedup				
AR	1.00x	1.00x	1.00x	1.00x	1.00x
EAGLE	1.60x	1.54x	1.47x	1.31x	1.14x
VSD	2.02x	1.79x	1.64x	1.49x	1.24x
PARD	3.06x	2.59x	2.19x	1.55x	1.17x

5 Related Work

Improving the inference efficiency of large language has been extensively studied from multiple perspectives. Quantization techniques such as GPTQ [14], AWQ [30], SmoothQuant [48], and LLM-QAT [34] focus on reducing computational and memory costs. To address long-context KV-cache management, approaches such as GQA [1], MLA [31], StreamingLLM [49], H2O [54], MoBA [36], and NSA [53] explicitly balances GPU memory consumption against model accuracy. At the system level, innovations like FlashAttention [10], FlashDecoding [22], MEGABLOCKS [16], and vLLM [24] deliver optimized kernels and scheduling strategies to maximize hardware utilization and throughput.

Speculative decoding [25] [6] improve GPU parallelism by leveraging a draft model to generate candidate tokens, which are then verified by the target model, achieving speedup without compromising

Table 5: Comparison of acceptance rates for PARD and EAGLE on LLaMA3-8B, where $k\text{-}\alpha$ denotes the average acceptance rate when the draft length is k .

Method	HumanEval		GSM8K	
	1- α	4- α	1- α	4- α
EAGLE	0.82	0.72	0.76	0.64
PARD	0.90	0.88	0.87	0.82

Table 6: Memory bandwidth usage during the draft phase of LLaMA3-8B model in bf16 dtype. PARD bandwidth usage remains constant as k increases.

Method	$k = 4$	$k = 6$	$k = 8$
	Draft BW Consumption		
EAGLE	5.94 GB	8.90 GB	11.88 GB
PARD	2.48 GB	2.48 GB	2.48 GB

accuracy. Other approaches such as LOOKAHEAD [15], PLD+ [43], REST [21] and SuffixDecoding [40] utilize text-based retrieval mechanisms to generate more informed drafts. LayerSkip [12], Kangaroo [33], and SWIFT [47] reuse selected layers of the target model to construct a lightweight draft model.

To improve the accuracy of speculative decoding, methods like Medusa [4], EAGLE [27], Amphista [28], Jakiro [23] and Hydra [2] incorporate representations from the target model as additional input signals. Approaches such as BiTA [18], ParallelSpec [50], and PaSS [39] introduce mask tokens to enable parallel speculative decoding. Further, techniques including Spectr [44], SpecInfer [38], Sequoia [8], and EAGLE-2 [27] optimize tree-based verification structures to enhance token acceptance rates.

6 Conclusion

In this work, we propose PARD, a novel speculative decoding framework that adapts the vanilla draft model into a parallel mode, significantly accelerating autoregressive generation while maintaining vanilla draft model accuracy. We introduce a conditional drop token strategy that speeds up training by over $3\times$. Our experiments demonstrate that PARD achieves a maximum $5.38\times$ speedup over optimized autoregressive decoding and an average $1.78\times$ improvement over vanilla speculative decoding. For Qwen2.5-7B, PARD reaches a peak throughput of **381** tokens per second on a single A100-40GB GPU. Additionally, PARD exhibits strong target independence, providing consistent acceleration across various model families, including LLaMA3, DeepSeek-R1, and Qwen. PARD establishes itself as a practical and effective approach for high-performance language model inference.

References

- [1] Joshua Ainslie, James Lee-Thorp, Michiel De Jong, Yury Zemlyanskiy, Federico Lebrón, and Sumit Sanghai. Gqa: Training generalized multi-query transformer models from multi-head checkpoints. *arXiv preprint arXiv:2305.13245*, 2023.
- [2] Zachary Ankner, Rishab Parthasarathy, Aniruddha Nrusimha, Christopher Rinard, Jonathan Ragan-Kelley, and William Brandon. Hydra: Sequentially-dependent draft heads for medusa decoding. *arXiv preprint arXiv:2402.05109*, 2024.
- [3] Tianle Cai, Yuhong Li, Zhengyang Geng, Hongwu Peng, Jason D. Lee, Deming Chen, and Tri Dao. Medusa: Simple llm inference acceleration framework with multiple decoding heads. *arXiv preprint arXiv:2401.10774*, 2024. to appear.
- [4] Tianle Cai, Yuhong Li, Zhengyang Geng, Hongwu Peng, Jason D Lee, Deming Chen, and Tri Dao. Medusa: Simple llm inference acceleration framework with multiple decoding heads. *arXiv preprint arXiv:2401.10774*, 2024.
- [5] Charlie Chen, Sébastien Borgeaud, Geoffrey Irving, Jean-Baptiste Lespiau, Laurent Sifre, and John Jumper. Accelerating large language model decoding with speculative sampling. *arXiv preprint arXiv:2302.01318*, 2023. DeepMind Technical Report.
- [6] Charlie Chen, Sébastien Borgeaud, Geoffrey Irving, Jean-Baptiste Lespiau, Laurent Sifre, and John Jumper. Accelerating large language model decoding with speculative sampling. *arXiv preprint arXiv:2302.01318*, 2023.
- [7] Mark Chen, Jerry Tworek, Heewoo Jun, Qiming Yuan, Henrique Ponde De Oliveira Pinto, Jared Kaplan, Harri Edwards, Yuri Burda, Nicholas Joseph, Greg Brockman, et al. Evaluating large language models trained on code. *arXiv preprint arXiv:2107.03374*, 2021.
- [8] Zhuoming Chen, Avner May, Ruslan Svirchevski, Yuhsun Huang, Max Ryabinin, Zhihao Jia, and Beidi Chen. Sequoia: Scalable, robust, and hardware-aware speculative decoding. *arXiv preprint arXiv:2402.12374*, 2024.
- [9] Karl Cobbe, Vineet Kosaraju, Mohammad Bavarian, Mark Chen, Heewoo Jun, Lukasz Kaiser, Matthias Plappert, Jerry Tworek, Jacob Hilton, Reiichiro Nakano, et al. Training verifiers to solve math word problems. *arXiv preprint arXiv:2110.14168*, 2021.

[10] Tri Dao, Dan Fu, Stefano Ermon, Atri Rudra, and Christopher Ré. Flashattention: Fast and memory-efficient exact attention with io-awareness. *Advances in neural information processing systems*, 35:16344–16359, 2022.

[11] DeepSeek-AI, Daya Guo, Dejian Yang, Haowei Zhang, Junxiao Song, Ruoyu Zhang, Runxin Xu, Qihao Zhu, Shirong Ma, Peiyi Wang, Xiao Bi, Xiaokang Zhang, Xingkai Yu, Yu Wu, Z. F. Wu, Zhibin Gou, Zhihong Shao, Zhuoshu Li, Ziyi Gao, Aixin Liu, Bing Xue, Bingxuan Wang, Bochao Wu, Bei Feng, Chengda Lu, Chenggang Zhao, Chengqi Deng, Chenyu Zhang, Chong Ruan, Damai Dai, Deli Chen, Dongjie Ji, Erhang Li, Fangyun Lin, Fucong Dai, Fuli Luo, Guangbo Hao, Guanting Chen, Guowei Li, H. Zhang, Han Bao, Hanwei Xu, Haocheng Wang, Honghui Ding, Huajian Xin, Huazuo Gao, Hui Qu, Hui Li, Jianzhong Guo, Jiashi Li, Jiawei Wang, Jingchang Chen, Jingyang Yuan, Junjie Qiu, Junlong Li, J. L. Cai, Jiaqi Ni, Jian Liang, Jin Chen, Kai Dong, Kai Hu, Kaige Gao, Kang Guan, Kexin Huang, Kuai Yu, Lean Wang, Lecong Zhang, Liang Zhao, Litong Wang, Liyue Zhang, Lei Xu, Leyi Xia, Mingchuan Zhang, Minghua Zhang, Minghui Tang, Meng Li, Miaojun Wang, Mingming Li, Ning Tian, Panpan Huang, Peng Zhang, Qiancheng Wang, Qinyu Chen, Qiushi Du, Ruiqi Ge, Ruisong Zhang, Ruizhe Pan, Runji Wang, R. J. Chen, R. L. Jin, Ruyi Chen, Shanghao Lu, Shangyan Zhou, Shanhua Chen, Shengfeng Ye, Shiyu Wang, Shuiping Yu, Shunfeng Zhou, Shuting Pan, S. S. Li, Shuang Zhou, Shaoqing Wu, Shengfeng Ye, Tao Yun, Tian Pei, Tianyu Sun, T. Wang, Wangding Zeng, Wanjia Zhao, Wen Liu, Wenfeng Liang, Wenjun Gao, Wenqin Yu, Wentao Zhang, W. L. Xiao, Wei An, Xiaodong Liu, Xiaohan Wang, Xiaokang Chen, Xiaotao Nie, Xin Cheng, Xin Liu, Xin Xie, Xingchao Liu, Xinyu Yang, Xinyuan Li, Xuecheng Su, Xuheng Lin, X. Q. Li, Xiangyue Jin, Xiaojin Shen, Xiaosha Chen, Xiaowen Sun, Xiaoxiang Wang, Xinnan Song, Xinyi Zhou, Xianzu Wang, Xinxia Shan, Y. K. Li, Y. Q. Wang, Y. X. Wei, Yang Zhang, Yanhong Xu, Yao Li, Yao Zhao, Yaofeng Sun, Yaohui Wang, Yi Yu, Yichao Zhang, Yifan Shi, Yiliang Xiong, Ying He, Yishi Piao, Yisong Wang, Yixuan Tan, Yiyang Ma, Yiyuan Liu, Yongqiang Guo, Yuan Ou, Yuduan Wang, Yue Gong, Yuheng Zou, Yujia He, Yunfan Xiong, Yuxiang Luo, Yuxiang You, Yuxuan Liu, Yuyang Zhou, Y. X. Zhu, Yanhong Xu, Yanping Huang, Yaohui Li, Yi Zheng, Yuchen Zhu, Yunxian Ma, Ying Tang, Yukun Zha, Yuting Yan, Z. Z. Ren, Zehui Ren, Zhangli Sha, Zhe Fu, Zhean Xu, Zhenda Xie, Zhengyan Zhang, Zhewen Hao, Zhicheng Ma, Zhigang Yan, Zhiyu Wu, Zihui Gu, Zijia Zhu, Zijun Liu, Zilin Li, Ziwei Xie, Ziyang Song, Zizheng Pan, Zhen Huang, Zhipeng Xu, Zhongyu Zhang, and Zhen Zhang. Deepseek-r1: Incentivizing reasoning capability in llms via reinforcement learning, 2025.

[12] Mostafa Elhoushi, Akshat Srivastava, Diana Liskovich, Basil Hosmer, Bram Wasti, Liangzhen Lai, Anas Mahmoud, Bilge Acun, Saurabh Agarwal, Ahmed Roman, Ahmed Aly, Beidi Chen, and Carole-Jean Wu. Layerskip: Enabling early exit inference and self-speculative decoding. In *Proceedings of the 62nd Annual Meeting of the Association for Computational Linguistics (Volume 1: Long Papers)*, page 12622–12642. Association for Computational Linguistics, 2024.

[13] Hugging Face. Open r1: A fully open reproduction of deepseek-r1, January 2025.

[14] Elias Frantar, Saleh Ashkboos, Torsten Hoefer, and Dan Alistarh. Gptq: Accurate post-training quantization for generative pre-trained transformers. *arXiv preprint arXiv:2210.17323*, 2022.

[15] Yichao Fu, Peter Bailis, Ion Stoica, and Hao Zhang. Break the sequential dependency of llm inference using lookahead decoding. *arXiv preprint arXiv:2402.02057*, 2024.

[16] Trevor Gale, Deepak Narayanan, Cliff Young, and Matei Zaharia. Megablocks: Efficient sparse training with mixture-of-experts. *Proceedings of Machine Learning and Systems*, 5:288–304, 2023.

[17] Marjan Ghazvininejad, Omer Levy, Yinhan Liu, and Luke Zettlemoyer. Mask-Predict: Parallel Decoding of Conditional Masked Language Models, September 2019. *arXiv:1904.09324 [cs]*.

[18] Fabian Gloeckle, Badr Youbi Idrissi, Baptiste Rozière, David Lopez-Paz, and Gabriel Synnaeve. Better and faster large language models via multi-token prediction, 2024. *arXiv:2404.19737*.

[19] Aaron Grattafiori, Abhimanyu Dubey, Abhinav Jauhri, Abhinav Pandey, Abhishek Kadian, Ahmad Al-Dahle, Aiesha Letman, Akhil Mathur, Alan Schelten, Alex Vaughan, et al. The llama 3 herd of models. *arXiv preprint arXiv:2407.21783*, 2024.

[20] Daya Guo, Dejian Yang, Haowei Zhang, Junxiao Song, Ruoyu Zhang, Runxin Xu, Qihao Zhu, Shirong Ma, Peiyi Wang, Xiao Bi, et al. Deepseek-r1: Incentivizing reasoning capability in llms via reinforcement learning. *arXiv preprint arXiv:2501.12948*, 2025.

[21] Zhenyu He, Zexuan Zhong, Tianle Cai, Jason D Lee, and Di He. Rest: Retrieval-based speculative decoding. *arXiv preprint arXiv:2311.08252*, 2023.

[22] Ke Hong, Guohao Dai, Jiaming Xu, Qiuli Mao, XiuHong Li, Jun Liu, Kangdi Chen, Yuhan Dong, and Yu Wang. Flashdecoding++: Faster large language model inference on gpus. *arXiv preprint arXiv:2311.01282*, 2023.

[23] Haiduo Huang, Fuwei Yang, Zhenhua Liu, Yixing Xu, Jinze Li, Yang Liu, Xuanwu Yin, Dong Li, Pengju Ren, and Emad Barsoum. Jakiro: Boosting speculative decoding with decoupled multi-head via moe. *arXiv preprint arXiv:2502.06282*, 2025.

[24] Woosuk Kwon, Zhuohan Li, Siyuan Zhuang, Ying Sheng, Lianmin Zheng, Cody Hao Yu, Joseph Gonzalez, Hao Zhang, and Ion Stoica. Efficient memory management for large language model serving with pagedattention. In *Proceedings of the 29th Symposium on Operating Systems Principles*, pages 611–626, 2023.

[25] Yaniv Leviathan, Matan Kalman, and Yossi Matias. Fast inference from transformers via speculative decoding. In *International Conference on Machine Learning*, pages 19274–19286. PMLR, 2023.

[26] Yuhui Li, Fangyun Wei, Chao Zhang, and Hongyang Zhang. EAGLE: Speculative sampling requires rethinking feature uncertainty. In *Proceedings of the 41st International Conference on Machine Learning (ICML)*, 2024. to appear.

[27] Yuhui Li, Fangyun Wei, Chao Zhang, and Hongyang Zhang. Eagle: Speculative sampling requires rethinking feature uncertainty. *arXiv preprint arXiv:2401.15077*, 2024.

[28] Zeping Li, Xinlong Yang, Ziheng Gao, Ji Liu, Guachen Li, Zhuang Liu, Dong Li, Jinzhang Peng, Lu Tian, and Emad Barsoum. Amphista: Bi-directional Multi-head Decoding for Accelerating LLM Inference, October 2024. *arXiv:2406.13170 [cs]*.

[29] Hunter Lightman, Vineet Kosaraju, Yura Burda, Harri Edwards, Bowen Baker, Teddy Lee, Jan Leike, John Schulman, Ilya Sutskever, and Karl Cobbe. Let’s verify step by step. *arXiv preprint arXiv:2305.20050*, 2023.

[30] Ji Lin, Jiaming Tang, Haotian Tang, Shang Yang, Wei-Ming Chen, Wei-Chen Wang, Guangxuan Xiao, Xingyu Dang, Chuang Gan, and Song Han. Awq: Activation-aware weight quantization for on-device llm compression and acceleration. *Proceedings of Machine Learning and Systems*, 6:87–100, 2024.

[31] Aixin Liu, Bei Feng, Bing Xue, Bingxuan Wang, Bochao Wu, Chengda Lu, Chenggang Zhao, Chengqi Deng, Chenyu Zhang, Chong Ruan, et al. Deepseek-v3 technical report. *arXiv preprint arXiv:2412.19437*, 2024.

[32] Cong Liu, Zhong Wang, Sheng Yu Shen, Jialiang Peng, Xiaoli Zhang, ZhenDong Du, and YaFang Wang. The chinese dataset distilled from deepseek-r1-671b. <https://huggingface.co/datasets/Congliu/Chinese-DeepSeek-R1-Distill-data-110k>, 2025.

[33] Fangcheng Liu, Yehui Tang, Zhenhua Liu, Yunsheng Ni, Kai Han, and Yunhe Wang. Kangaroo: Lossless self-speculative decoding via double early exiting. *arXiv preprint arXiv:2404.18911*, 2024.

[34] Zechun Liu, Barlas Oguz, Changsheng Zhao, Ernie Chang, Pierre Stock, Yashar Mehdad, Yangyang Shi, Raghuraman Krishnamoorthi, and Vikas Chandra. Llm-qat: Data-free quantization aware training for large language models. *arXiv preprint arXiv:2305.17888*, 2023.

[35] AI @ Meta Llama Team. The llama 3 herd of models, 2024.

[36] Enzhe Lu, Zhejun Jiang, Jingyuan Liu, Yulun Du, Tao Jiang, Chao Hong, Shaowei Liu, Weiran He, Enming Yuan, Yuzhi Wang, et al. MoBA: Mixture of block attention for long-context llms. *arXiv preprint arXiv:2502.13189*, 2025.

[37] Ziyang Luo, Can Xu, Pu Zhao, Qingfeng Sun, Xiubo Geng, Wenxiang Hu, Chongyang Tao, Jing Ma, Qingwei Lin, and Daxin Jiang. Wizardcoder: Empowering code large language models with evol-instruct, 2023.

[38] Xupeng Miao, Gabriele Oliaro, Zhihao Zhang, Xinhao Cheng, Zeyu Wang, Zhengxin Zhang, Rae Ying Yee Wong, Alan Zhu, Lijie Yang, Xiaoxiang Shi, et al. Specinfer: Accelerating generative large language model serving with tree-based speculative inference and verification. *arXiv preprint arXiv:2305.09781*, 2023.

[39] Giovanni Monea, Armand Joulin, and Edouard Grave. Pass: Parallel speculative sampling. *arXiv preprint arXiv:2311.13581*, 2023.

[40] Gabriele Oliaro, Zhihao Jia, Daniel Campos, and Aurick Qiao. Suffixdecoding: A model-free approach to speeding up large language model inference. *arXiv preprint arXiv:2411.04975*, 2024.

[41] OpenAI. Gpt-4 technical report, 2023.

[42] Alec Radford, Karthik Narasimhan, Tim Salimans, Ilya Sutskever, et al. Improving language understanding by generative pre-training, 2018.

[43] Shwetha Somasundaram, Anirudh Phukan, and Apoorv Saxena. Pld+: Accelerating llm inference by leveraging language model artifacts. *arXiv preprint arXiv:2412.01447*, 2024.

[44] Ziteng Sun, Ananda Theertha Suresh, Jae Hun Ro, Ahmad Beirami, Himanshu Jain, and Felix Yu. Spectr: Fast speculative decoding via optimal transport. *Advances in Neural Information Processing Systems*, 36:30222–30242, 2023.

[45] OpenThoughts Team. Open Thoughts. <https://open-thoughts.ai>, January 2025.

[46] T Wolf. Huggingface’s transformers: State-of-the-art natural language processing. *arXiv preprint arXiv:1910.03771*, 2019.

[47] Heming Xia, Yongqi Li, Jun Zhang, Cunxiao Du, and Wenjie Li. Swift: On-the-fly self-speculative decoding for llm inference acceleration. *arXiv preprint arXiv:2410.06916*, 2024.

[48] Guangxuan Xiao, Ji Lin, Mickael Seznec, Hao Wu, Julien Demouth, and Song Han. Smoothquant: Accurate and efficient post-training quantization for large language models. In *International Conference on Machine Learning*, pages 38087–38099. PMLR, 2023.

[49] Guangxuan Xiao, Yuandong Tian, Beidi Chen, Song Han, and Mike Lewis. Efficient streaming language models with attention sinks. *arXiv preprint arXiv:2309.17453*, 2023.

[50] Zilin Xiao, Hongming Zhang, Tao Ge, Siru Ouyang, Vicente Ordonez, and Dong Yu. ParallelSpec: Parallel drafter for efficient speculative decoding. *arXiv preprint arXiv:2408.06421*, 2024.

[51] Zhangchen Xu, Fengqing Jiang, Luyao Niu, Yuntian Deng, Radha Poovendran, Yejin Choi, and Bill Yuchen Lin. Magpie: Alignment data synthesis from scratch by prompting aligned llms with nothing. *arXiv preprint arXiv:2406.08464*, 2024.

[52] An Yang, Baosong Yang, Beichen Zhang, Binyuan Hui, Bo Zheng, Bowen Yu, Chengyuan Li, Dayiheng Liu, Fei Huang, Haoran Wei, et al. Qwen2. 5 technical report. *arXiv preprint arXiv:2412.15115*, 2024.

[53] Jingyang Yuan, Huazuo Gao, Damai Dai, Junyu Luo, Liang Zhao, Zhengyan Zhang, Zhenda Xie, YX Wei, Lean Wang, Zhiping Xiao, et al. Native sparse attention: Hardware-aligned and natively trainable sparse attention. *arXiv preprint arXiv:2502.11089*, 2025.

[54] Zhenyu Zhang, Ying Sheng, Tianyi Zhou, Tianlong Chen, Lianmin Zheng, Ruisi Cai, Zhao Song, Yuandong Tian, Christopher Ré, Clark Barrett, et al. H2o: Heavy-hitter oracle for efficient generative inference of large language models. *Advances in Neural Information Processing Systems*, 36:34661–34710, 2023.

A Appendix

Speedup on MI250X: Table 7 reports results on MI250X, showing that PARD achieves consistent speedup across different devices.

Table 7: Speedup comparison of AR Draft and PARD across different series models on MI250X.

Series	Target	Method	Draft	MATH500		GSM8k	Average
				Speedup	Speedup		
L3	L32 3B	AR Draft	L32 1B	1.39	1.45	1.33	1.39
		PARD	L32 1B PARD	2.32	2.54	2.14	2.33
DSQ	L31 8B	AR Draft	L32 1B	2.01	2.13	1.99	2.04
		PARD	L32 1B PARD	2.69	3.30	2.68	2.89
DSQ	DSQ 7B	AR Draft	DSQ 1.5B	1.51	1.38	1.51	1.47
		PARD	DSQ 1.5B PARD	2.77	2.12	2.53	2.47
DSQ	DSQ 14B	AR Draft	DSQ 1.5B	2.43	2.12	2.45	2.33
		PARD	DSQ 1.5B PARD	3.64	2.58	3.17	3.13
Qwen	Q2 7B	AR Draft	Q2.5 0.5B	1.89	1.99	1.93	1.93
		PARD	Q2.5 0.5B PARD	2.74	3.49	2.99	3.07
Qwen	Q2.5 1.5B	AR Draft	Q2.5 0.5B	1.14	1.11	1.16	1.14
		PARD	Q2.5 0.5B PARD	2.72	2.78	2.74	2.75
Qwen	Q2.5 3B	AR Draft	Q2.5 0.5B	1.55	1.50	1.61	1.55
		PARD	Q2.5 0.5B PARD	2.94	3.50	3.43	3.29
Qwen	Q2.5 7B	AR Draft	Q2.5 0.5B	2.29	2.09	2.31	2.23
		PARD	Q2.5 0.5B PARD	3.84	4.30	4.48	4.21
Qwen	Q2.5 14B	AR Draft	Q2.5 0.5B	3.37	3.19	3.53	3.36
		PARD	Q2.5 0.5B PARD	4.31	4.87	5.12	4.77
Qwen	Q2.5 7B 1M	AR Draft	Q2.5 0.5B	2.24	2.08	2.39	2.24
		PARD	Q2.5 0.5B PARD	3.66	3.76	4.16	3.86